Solar Energy Materials & Solar Cells 281 (2025) 113316

Contents lists available at ScienceDirect

Solar Energy Materials and Solar Cells

journal homepage: www.elsevier.com/locate/solmat

Thermal and environmental durability of novel particles for Concentrated solar thermal technologies

Florian Sutter [a,*], Gözde Alkan [b], Nassira Benameur [c], Samuel Marlin [c], Gema San Vicente [d], Angel Morales [d], Tomás Jesus Reche Navarro [a], Ana Cleia González Alves [a], Lucía Martínez Arcos [d], Daniel Benítez [a], Aránzazu Fernández-García [d], Ceyhun Oskay [e], Christoph Grimme [e]

[a] German Aerospace Center DLR, Institute of Solar Research, Calle Doctor Carracido Nr. 44, 1st floor, 04005, Almería, Spain
[b] German Aerospace Center DLR, Institute of Materials Research, Linder Höhe, 51147, Cologne, Germany
[c] Saint-Gobain Research Provence, Avenue Alphonse Jauffret 550, CS 20224 - F 84306 Cavaillon Cedex, France
[d] CIEMAT-Plataforma Solar de Almería, Carretera de Senés, km. 4.5, P.O. Box 22, E04200 Tabernas, Spain
[e] DECHEMA-Forschungsinstitut, High Temperature Materials, Theodor-Heuss-Allee 25, 60486, Frankfurt am Main, Germany

ARTICLE INFO

Keywords:
Concentrated solar power
Particle
Coating
Aging testing
Solar absorptance
Thermal emittance

ABSTRACT

Bauxite-based proppants, commonly used in the fracking industry, are also employed in solid particle receiver types of Concentrated Solar Thermal (CST) technologies. However, fracking has been banned in many countries due to its environmental impact, leading to a decline in demand for proppants. As a result, the current proppant price of 1 €/kg is expected to rise due to reduced production capacities. Therefore, alternative particle types need to be developed for Concentrated Solar Thermal applications.

Cost-effective particle production compared to traditional bauxite sintering has been explored. In this study, we conduct long-term isothermal aging tests at 1000 °C up to 4000 h to assess the optical degradation of novel cost-effective particles, which are composed almost entirely of recycled waste products. The performance of these novel particles is compared to traditional proppants. Additionally, we examine the durability of three types of coatings designed to enhance the solar absorptance of the particles from approximately 83 %–97.5 %. These coated particles are also subjected to climate chamber tests under controlled humidity and freezing conditions to determine if environmental factors will degrade the coatings.

Nomenclature and abbreviations

α_s	solar absorptance	[−]
$c_{p,1000°C}$	specific heat capacity at 1000 °C	[J/(g K)]
ε_t	thermal emittance	[−]
F_b	breaking force	[N]
HV 0.1	Vickers Hardness according to ISO6507 method 0.1	[−]
η	opto-thermal efficiency of the particles	[−]
λ	wavelength	[nm]
ρ_b	Bulk density	[g/cm^3]
t	testing time	[h]
T	temperature	[°C]
T_s	softening temperature	[°C]
CIE	Centro de Investigaciones Energéticas, Medioambientales y Tecnológicas	
CSP	Concentrated Solar Power	
CST	Concentrated Solar Thermal technologies	
DFI	Dechema-Forschungsinstitut	
DLR	German Aerospace Center	
EDS	Energy-dispersive X-ray microanalysis	
RAM	Resonance Acoustic Mixer	
SEM	Scanning electron microscopy	

1. Introduction

CST technologies hold immense potential for sustainable energy production, offering a reliable source of electricity or heat with minimal environmental impact. In recent years, the integration of solid particles

* Corresponding author.
E-mail address: Florian.Sutter@dlr.de (F. Sutter).

https://doi.org/10.1016/j.solmat.2024.113316
Received 23 July 2024; Received in revised form 24 October 2024; Accepted 20 November 2024
Available online 27 November 2024

into Concentrated Solar Power (CSP) towers has emerged as a promising solution to potentially increase the thermal efficiencies due to the ability to operate at higher temperatures. Solid particles can absorb solar radiation and store thermal energy effectively overcoming the main issues related to the state-of-the-art heat transfer medium solar salt: corrosion, thermal decomposition and solidification [1].

The initial concept of a solar particle receiver originated in the 1980s at Sandia National Laboratories [2]. Since then, several receiver concepts have been developed and tested, mainly reaching particle temperatures in the range between 700 and 1000 °C. A good summary of the different receiver concepts can be found in Refs. [3,4].

Several material types have been studied as candidate heat transfer and storage particles for CSP plants. The most commonly utilized material is sintered bauxite, developed to provide structural support in fractured oil and gas wells (known as "proppants" [5]). Proppants possess remarkable strength, along with non-corrosive properties, cost-effectiveness, and wide availability in formulations with good solar absorptance. Predominantly comprising sintered bauxite, proppants vary primarily in alumina-to-silica ratio and the presence of other oxide components. Nevertheless, proppants in their original state are not stable when subjected to oxidizing conditions. They undergo a color alteration and a corresponding decrease in solar absorptance (α_s) when exposed to temperatures above 700 °C for several hours in an air environment. In the past 10 years a couple of studies have been published to assess the durability of different particle types ([6–12]).

Siegel et al. presented in Ref. [6] the evolution of α_s and thermal emittance (ε_t) for three commercially available proppant materials from CARBO ceramics when heated isothermally in air to 700 and 1000 °C for up to 192 h. The solar absorptance was stable at 700 °C but not at 1000 °C, showing a decrease from 91 % to 84 % for CARBOHSP®. X-ray diffraction investigation revealed phase transformation leading to the reduction of solar absorptance. In Ref. [7] the same authors have shown that the undesirable change in solar absorptance may be reversed through chemical reduction in forming gas at a temperature above 700 °C.

CARBOHSP® particles were also studied under thermocyclic conditions in Ref. [8]. Calderón et al. confirmed that those particles are affected by isothermal temperature aging due to surface chemical composition. They found good durability of CARBOHSP® under cyclic conditions between 300 and 900 °C. The behavior was opposite for black silicon carbide particles, which were rather affected by thermal cycling than by constant temperature aging.

The group around Palacios [9] has conducted isothermal aging experiments at 750 and 900 °C of black silicon carbide, silica sand and iron oxide particles. The black silicon carbide particles showed the best optical behavior out of the three candidates, reaching 96 % solar absorptance after 500 h of testing. However, the cost of black silicon carbide particles, estimated at 13–18.6 €/kg in Ref. [8], is prohibitively high.

A considerably more economical solution is to use natural granular materials. Some thermophysical properties of natural granulates and technical ceramic bulk materials have been reported in Ref. [10]. The tested ceramics demonstrated high resistance to thermal shock, whereas the natural products exhibited pronounced degradation. Materials containing quartz phases are vulnerable to rapid temperature changes due to quartz inversion (phase transition from alpha-to beta-quartz at 573 °C). On the other hand, bauxite generated a large amount of debris during attrition testing in their shear cell.

In [11] desert dune sand from different locations of the United Arab Emirates were collected and studied as thermal energy storage material. They found that the transformation of calcium carbonate into calcium oxide during thermal aging at 1000 °C for 8 h had a negative impact on the solar absorptance of the sand. The solar absorptance of the collected sand samples was quite low, ranging from 50 to 59 % after thermal aging for 8 h.

In [12] various types of particles were exposed to 350 and 950 °C up to 10 days and the evolution of reflectance and emittance was measured with a handheld reflectometer and emissometer. The particle samples included in the study were two natural sands from Saudi Arabia, CARBOHSP® sintered bauxite proppants, two batches of alumina-based Carbo-Accucast ID50-K, industrial sand from Atlanta Sand and Supply Company, fracking sands from Saudi Arabia, Southern Ohio and from Preferred Sand Company. It was found that most particles showed a decrease in α_s and ε_t and that these changes of optical properties occurred within the first 24 h of exposure to 950 °C. Only one of the Saudi Arabia natural sands and the Saudi Arabia fracking sand showed constant α_s values. However, those particles had insufficient initial values. They concluded that the changes are large enough to affect the receiver efficiency and that particles with more stable solar absorptance should be developed with high priority.

It is common practice in CSP systems to enhance the solar absorptance by applying specific absorber coatings. In the low to mid temperature range (<400 °C) the utilized coatings are usually selective; thus, their low thermal emittance allows to minimize heat losses of the receiver [13] [14],. Although some candidate selective coatings exist for elevated temperatures (600 °C in Ref. [15] and 650 °C in Ref. [16]), absorber coatings for commercial applications are typically non-selective with the aim to favor durability over opto-thermal performance (examples of non-selective coatings can be found in Refs. [17, 18]).

Few studies in the literature have reported coatings for particles; however, none of the existing particle receiver demonstrators currently utilize coated particles. In Ref. [19], particles were dip-coated in Pyromark 2500 high temperature paint, which is the commonly used paint for tubular solar tower absorbers. The coating turned out to be not sufficiently mechanically stable. Furthermore, coloring diffusion treatments were tried and the solar absorptance was raised from 87 % to 95 %. It was also tried to color the proppant raw material with 10 % of commercially available "Pigment Black 26", revealing a solar absorptance of about 90 %. The latter method is believed to be more cost-effective, compared to the expensive diffusion process.

In [20], manganese iron black (PBK26) coatings were prepared for quartz, bauxite and mullite substrate particles by water bath method and the performance was found to be the best when Fe/Mn molar ratio in PBK26 was 4:1. The coated particles were tested under isothermal and cyclic furnace exposure, as well as in a wear test. Although some mass loss was measured after the experiments, it was concluded that the PBK26 coating significantly improves the absorptance of the particles and that the stability of the coating is promising.

During operation, the hot ceramic particles move along the inner receiver surfaces, outlet duct and heat exchanger tubes or other system components (storage container, etc.). Studies like [21,22] revealed relevant erosion rates of the utilized metallic construction materials. However, the conducted attrition test in Ref. [23] concludes that rate of attrition (= reduction of particle diameter) or loss of particles is expected to be insignificant over the life of the CSP system. Wear due to interaction with metallic walls or other particles is a potential issue for coating durability, which has not been sufficiently addressed yet.

In this study, we examine the durability of novel particles developed by Saint-Gobain and corresponding coatings developed by DLR, CIE and DFI. The conducted isothermal testing campaign reaches a duration of 4000 h, largely exceeding the previously reviewed studies. In addition, we conduct climatic chamber tests to examine the effect of environmental stressors like humidity or freezing conditions on the coating performance. To our knowledge, these kinds of tests have not been reported before in literature.

2. Material and methods

This section includes a description of the particle materials used in this study, the methodology followed to analyze their durability under accelerated aging conditions and the evaluation techniques employed to determine their behavior.

Table 1
Chemistry of state-of-the-art proppants in wt-%.

Material code	Al_2O_3	SiO_2	Fe_2O_3
SB 30/50	>75	<10	>5
BL 30/50 and BL 16/30	>65	<18	>5
IP 30/50	55–60	<20	<9

2.1. Particle samples

Four previously commercial proppant types were delivered by Saint-Gobain: sintered bauxite (SB 30/50), BauxLite (in two size distributions, BL 16/30 and BL 30/50) and InterProp (IP 30/50). The main components of their chemical composition are Al_2O_3, SiO_2 and Fe_2O_3 (see Table 1). The size of the particles ranges from 297 to 590 μm for the 30/50 grades and from 590 to 1190 μm for the 16/30 grade. The proppants show an excellent roundness and sphericity, high hardness, softening temperature between 850 and 882 °C, bulk density of 1.6–1.9 g/cm^3, high specific heat capacity of 1.1–1.3 J/(g·K) at 1000 °C, solar absorptance of 83–91 % and low cost (see Table 2). After ceasing proppant production in 2020, Saint-Gobain examined alternative particles for CSP application. The first route, manufacturing of aluminum-oxide-rich particles was achieved via a fusion process, offering excellent solar absorptance of more than 97 %, superior roundness and sphericity, higher hardness and bulk density compared to state-of-the-art proppants. Two generations of fused particles were included in the testing. However, the fused particles were discarded for commercialization due to estimated manufacturing costs of about 3–5 €/kg. The second route was based on an iron-rich particle type composed by a mix of different oxides. The particles are produced via the granulation process with recycled waste products from the steel industry. Hence, low cost of around 1 € per kg can be achieved. Four generations of granulated particles were developed (Gen 1-4), of which only Gen2-4 were included in the testing. Mechanical resistance has been improved along the generations, ultimately matching the breaking force of the state-of-the-art proppants. However, this improvement came at the price of a reduction in solar absorptance down to 83 % for Gen4, still at the approximate same level of state-of-the-art bauxite particles. Overall, Gen4 particles present the best compromise in terms of cost and performance and were identified as promising commercial solution. The main components of the chemical composition of Gen4 particles are Al_2O_3 (>30 wt-%), Fe_2O_3 (<30 wt-%), SiO_2 (<20 wt-%), ZrO_2 (>20 wt-%) and others (~5 wt-%).

This study includes three novel types of coatings, developed by DLR, CIE and DFI, respectively. Coated Gen3 and Gen4 particles have been included in the isothermal experiments. For the climatic chamber tests, only coated Gen4 particles have been examined.

DLR employed a dry powder coating method, using a resonance acoustic mixer (RAM, Resodyn, Butte, MT, USA), details of this method can be found elsewhere [24,25]. Deep-black (Kremer Pigmente GmbH & Co. KG, Aichstetten, Germany), a commercial spinel type pigment, (CuMnFeOx) was utilized to blacken Gen3 and Gen4 particles. The coating process was performed by high-energy, high-speed mixing of particles and small quantities of spinel powders in a RAM. Thanks to the electrostatic attraction, deep black powder deposited on particle surfaces. Subsequent sintering at 1200 °C for 2 h beyond the spinel melting temperature ensured the integration of the coating layer to the particle surface. The solar absorptance reached is in the range of 92–93 %.

The coating developed by CIE is applied through a dip-coating-like process, using a $CuCoMnO_x$ precursor solution with SiO_2 nanoparticles. The precursor solutions were prepared by dissolving in absolute ethanol the precursors of copper nitrate (Sigma Aldrich, 98–103 %),

Table 2
Material codes and properties of the particles included in the study.

	Material code	Chemical composition	α_s [−]	ε_t [−]	ρ_b [g/cm^3]	T_s [°C]	F_b [N]	*HV 0.1* [−]	$c_{p,1000°C}$ [J/(g K)]	Cost [€/kg]
Fracking proppants	*SB 30/50*	Al_2O_3-rich	0.845	0.757	1.9	882	N/A	911	1.3	<1.5
	BL 16/30	Al_2O_3-rich	0.914	0.845	1.7	857	141	833	1.2	<1.5
	BL 30/50	Al_2O_3-rich	0.851	0.767	1.6	850	N/A	623	1.1	<1.5
	IP 30/50	Al_2O_3-rich	0.834	0.737	1.7	856	N/A	723	1.1	<1.5
Novel particles	*Fused_1*	Mix of oxides	0.964	0.951	2.1	1110	63	1110	1.2	5
	Fused_2	Mix of oxides	0.974	0.941	2.1	1080	98	988	N/A	3
	Gen2	Fe_2O_3-rich	0.928	0.829	2.8	1010	70	636	0.9	3
	Gen3	Fe_2O_3-rich	0.882	0.772	2.8	1080	90	704	0.9	1.3–1.5
	Gen4	Fe_2O_3-rich	0.833	0.614	2.0	940	120–140	926	1.1	~1
Coated particles	*Gen3_DLR*	Cu-Mn-Fe spinel	0.925	0.757	2.8	1080	90	704	0.9	~2
	Gen3_CIE	Cu-Mn-Co spinel	0.975	0.864	2.8	1080	90	704	0.9	~2
	Gen3_DFI	Cu-Cr spinel	0.963	0.908	2.8	1080	90	704	0.9	~2
	Gen4_DLR	Cu-Mn-Fe spinel	0.926	0.708	2.0	940	120–140	926	1.1	~1.6
	Gen4_CIE	Cu-Mn-Co spinel	0.967	0.809	2.0	940	120–140	926	1.1	~1.6
	Gen4_DFI	Cu-Cr spinel	0.970	0.931	2.0	940	120–140	926	1.1	~1.6

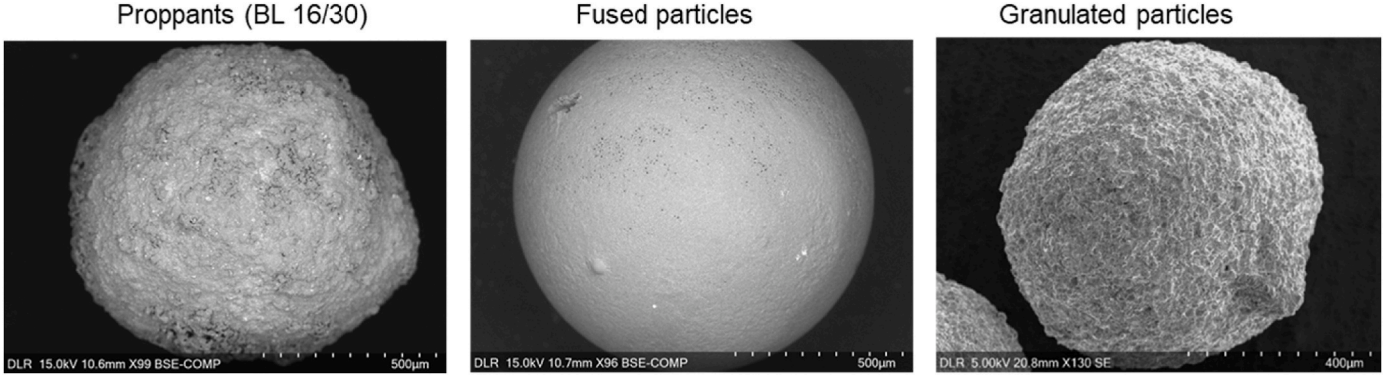

Fig. 1. SEM images of the surface of representative particles.

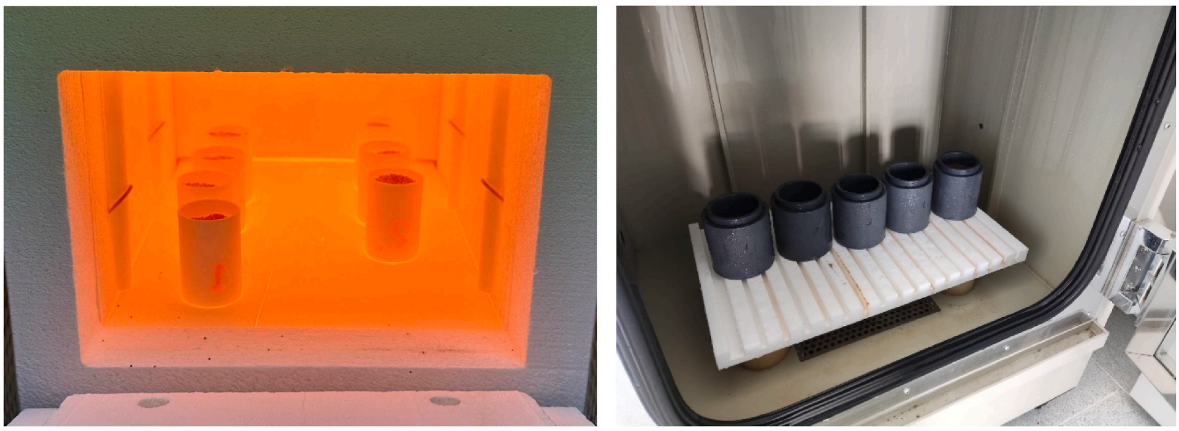

Fig. 2. Exposure of some particle types to 1000 °C in alumina crucibles in muffle furnace (left) and in climatic chambers to humidity conditions (right).

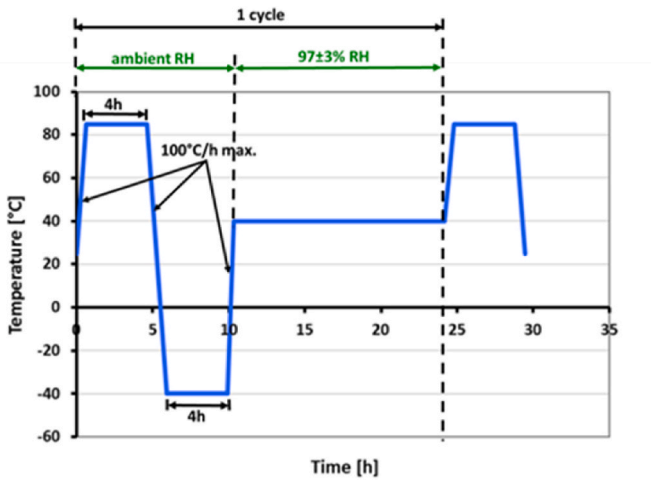

Fig. 3. Steps of the cyclic exposure test according to UNE206016:2018, Test 6.8, Method A.

cobalt nitrate (PRS Panreac, 98 %) and manganese nitrate (PRS Panreac, 98 %) in a molar ratio of 1:0.6:1 and adding a complexing agent and a wetting additive to improve film adhesion. 15 % colloidal silica (Aerosil® 792) was incorporated after salts dissolution. The precursor solution is poured on the particles then drained by gravity and the resulting coated particles are introduced into the oven at 1000 °C for 2 h. More details about the preparation and characterization of this coating can be found in Ref. [26]. High solar absorptance up to 97.5 % was achieved.

The coating developed by DFI is applied by air-spraying an ethanol-based suspension containing the Silikophen® AC900 resin (Evonik Industries), rheological additives, hardening agents and Heucodur® Black 9–100 (Heubach GmbH) $CuCr_2O_4$ black pigments. The coating thickness is between 15 and 40 μm and it is cured at room temperature which leads to the fine dispersion of copper chromite pigments in a silica matrix. High solar absorptance up to 97 % was achieved.

Table 2 summarizes relevant properties of the included particle types in this study. Fig. 1 shows how they differ in surface characteristics: whilst fused particles are very smooth and they exhibit a high roundness, proppants and granulated particles show higher surface roughness and more irregular shapes.

2.2. Testing conditions

The particle materials described in the previous section were submitted to three type of accelerated aging tests. The first one (thermal exposure test) is focused on simulating the extreme temperature during operation, while the second and third ones (environmental exposure tests) are designed to emulate ambient conditions that might be suffered by the particles during plant down time during maintenance periods.

2.2.1. Thermal exposure test

100 g of each particle type listed in Table 2 were exposed in a Nabertherm LT 40/12 muffle furnace for long-term high temperature

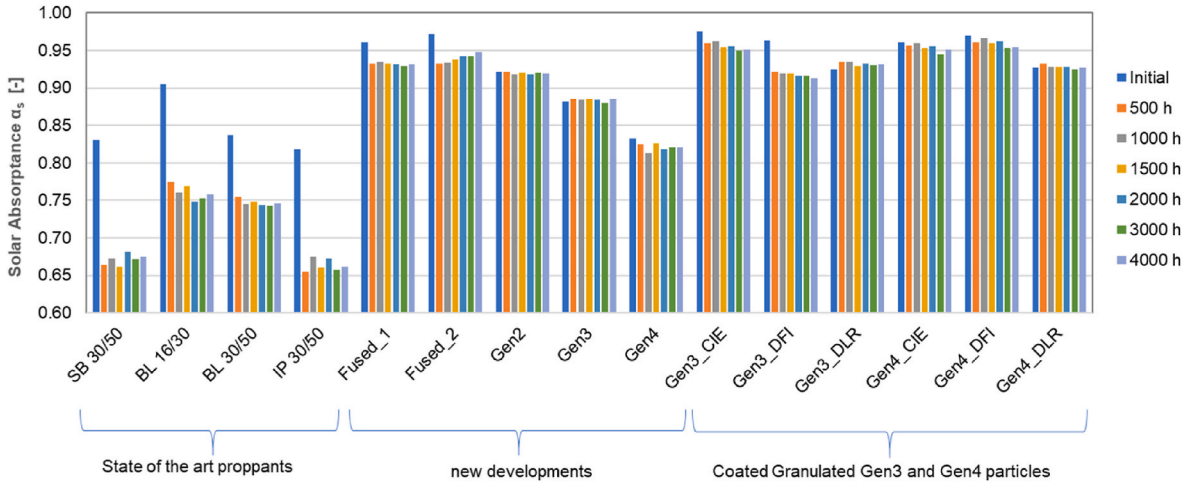

Fig. 4. Solar absorptance of the different particle types during exposure up to 4000 h to 1000 °C.

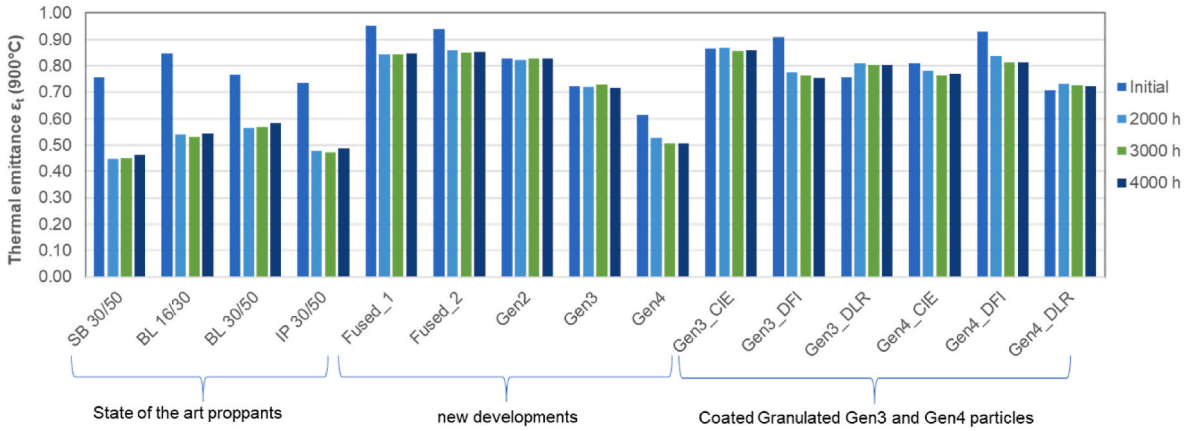

Fig. 5. Thermal emittance at 900 °C of the different particle types during exposure up to 4000 h to 1000 °C.

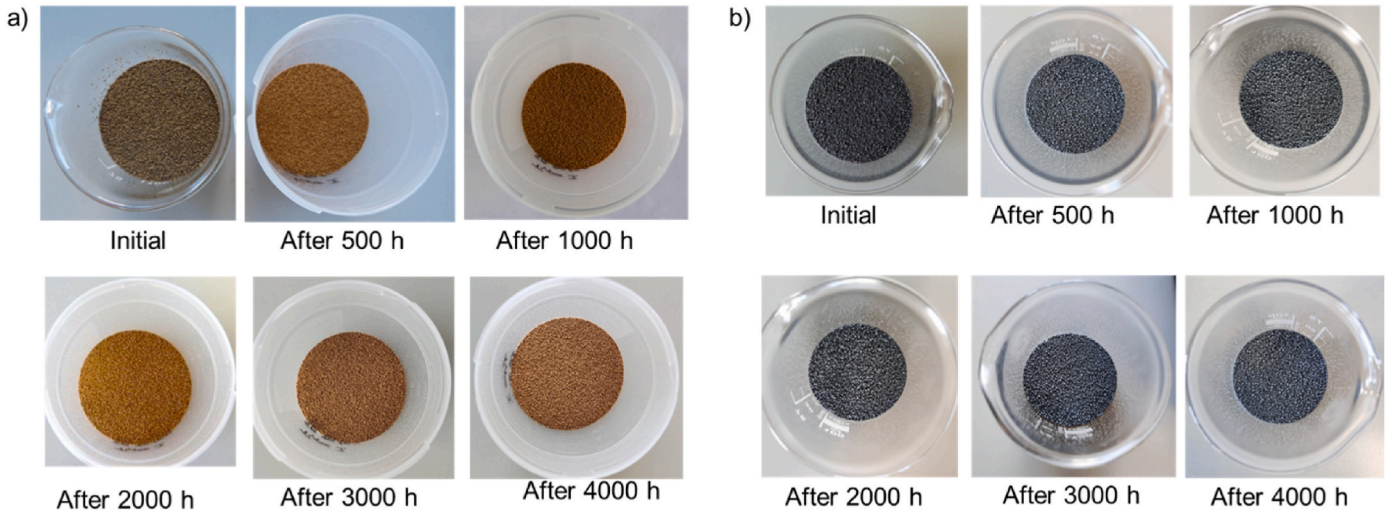

Fig. 6. Visual evolution of SB 30/50 proppants (a) and granulated Gen3 particles (b) throughout the test.

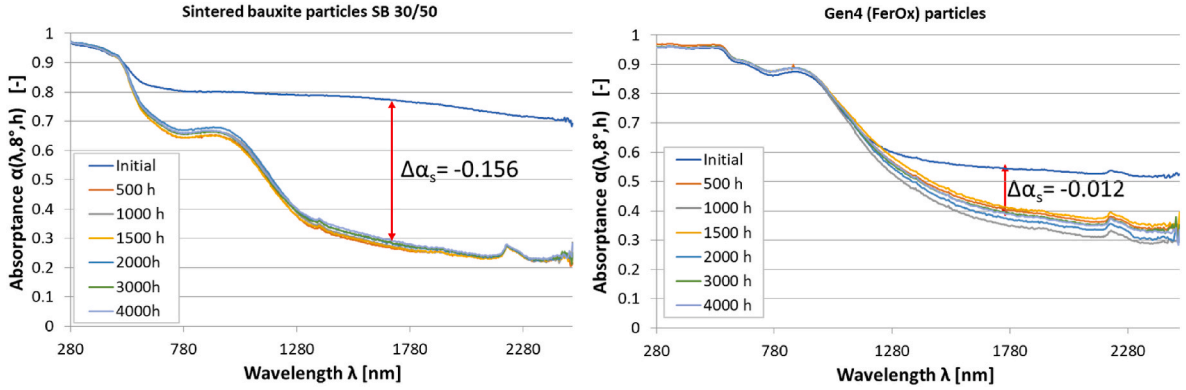

Fig. 7. Spectral absorptance change during exposure of state-of-the-art sintered bauxite particles SB 30/50 (left) and Gen4 particles (right) to 1000 °C for 4000 h.

testing up to 4000 h. The test is conducted at 1000 °C. The particles have been placed in alumina crucibles in the furnace (see Fig. 2 a). The test was interrupted each 500 h for intermediate optical characterization of the particles. After 3400 and 4000 h, few particles were extracted for SEM and EDS analysis.

2.2.2. *Environmental exposure tests*

Again, 100 g of pristine particles were exposed in two different climatic chambers to check their interaction at prolonged times with humidity and under cyclic freezing conditions. The two conducted environmental tests are standardized in ISO 6270–2, Test CH (named as condensation test) [27] and UNE206016:2018, Test 6.8, Method A (named as cyclic exposure test) [28].

The condensation test consisted of exposing the particle samples to constant conditions of 100 % relative humidity at 40 °C. The test was conducted for 960 h. The particles were introduced in small plastic

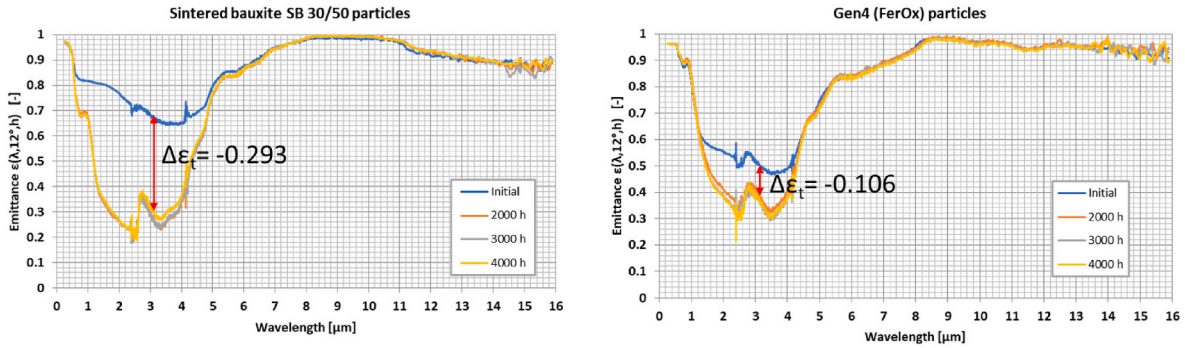

Fig. 8. Spectral emittance change during exposure of state-of-the-art sintered bauxite particles SB30/50 (left) and Gen4 particles (right) to 1000 °C for 4000 h.

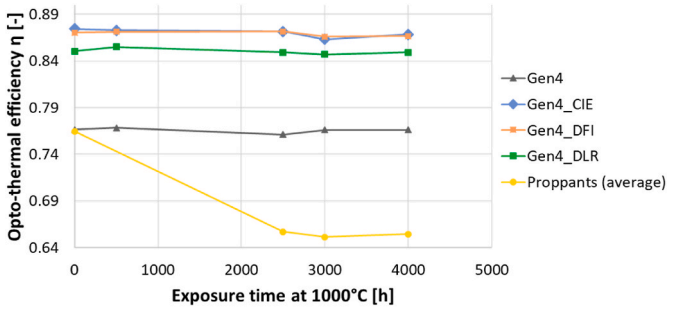

Fig. 9. Evolution of the opto-thermal efficiency during exposure to 1000 °C for selected particle types.

vessels with a filter in the bottom to avoid stagnant water through condensed humidity (see Fig. 2 b).

Each cycle of the cyclic exposure test consisted in the following steps (see also Fig. 3):

- 4 h at 85 °C
- 4 h at −40 °C (applying a maximum cooling rate of 100 °C/h)
- Approx. 16 h at 40 °C and 97 % of relative humidity

The test was conducted for 40 cycles, corresponding to a total testing time of 960 h. The same plastic vessels with filter to avoid stagnant water were used to place the particles in the chamber.

Not all of the particle types listed in Table 2 were included in the environmental exposure tests. Both tests were only conducted on Gen 4 particles and their coatings, as well as on SB 30/50 proppants as reference.

2.3. Characterization techniques

Measuring the optical properties of particles has the difficulty that typical spectrometers require vertical sample positioning. In this case, the measurement of the particle film needs to be accomplished through a window. The methodology of applying a window-correction to the measured data has been first described in Ref. [19]. This correction formula has been discussed and slightly modified within a group of optical experts under the SolarPaces TaskIII framework. A result of this discussion is the published guideline on how to measure solar absorptance and thermal emittance of particles [29]. A round robin test among seven laboratories validates the method [30].

For the herein conducted study, a *PerkinElmer Lambda* 1050 UV/VIS/NIR spectrophotometer with a 150 mm integrating sphere was used to measure reflectance in the range of 280–2500 nm. The reflectance of the particles was measured through a 1 mm quartz glass window and the spectral absorptance of the particles was computed following the window-correction method described in Ref. [29]. The α_s of the particles was computed by weighting the spectral absorptance data with the direct normal spectral irradiance reported in IEC 60904–3:2019 [31]. The measurement was conducted at an incidence angle of 8°.

The emittance data in the range between 2 and 16 µm was collected using a *PerkinElmer Frontier CSI* spectrometer with a 76 mm gold-coated *Mid-IR IntegratIR* integrating sphere from *Pike Technologies*. The reflectance of the particles was measured through a 2 mm ZnSe window with anti-reflective coating. The spectral absorptance of the particles was computed following [29]. In order to compute the ε_t of the particles, the absorptance spectrum was weighted with the black body spectrum at 900 °C (which is the targeted operation temperature of the particles). The measurement was conducted at an incidence angle of 12°.

Both values, α_s and ε_t, are used to compute the opto-thermal efficiency η, which is a figure of merit for absorber materials [16]. η is computed according to the following equation:

$$\eta = \frac{\alpha_s \bullet Q - \varepsilon_t \bullet \sigma \bullet T^4}{Q} \quad (1)$$

where Q is the targeted solar flux of 1000 kW/m^2, T the targeted temperature of the particles of 900 °C and σ the Stefan-Boltzmann constant of 5.67•10^{-8} W m^{-2} K^{-4}.

Microstructural and chemical analysis were performed by scanning electron microscopy (Ultra 55, Zeiss, Germany) and energy-dispersive spectroscopy (EDS; UltiMate, Oxford, UK). Prior to SEM analysis, particles were prepared metallographically, embedding them into hot mounting powder EOP black (ATM Qness GmbH, Germany) at 160 °C and 100 bar in a mounting press (Struers, CitoPress-30, Germany). Afterwards cross-sections were ground and polished. Surface investigations of the particles were performed by SEM in low vacuum condition (SU 3800, Hitachi High-Tech Europe, Krefeld, Germany).

Light-microscopic images were recorded with a Leica M205C encoded stereo microscope.

3. Results and discussion

3.1. Thermal exposure test

The results of the evolution of the solar absorptance and the thermal emittance throughout the thermal exposure test are shown in Figs. 4 and 5.

In accordance to the thermal exposure tests conducted in Ref. [6] [8, 12], it was found that proppants undergo a color change when exposed to temperatures of 1000 °C. Fig. 6 shows that the α_s change happens within the first 500 h of exposure for all four studied state-of-the-art proppant types. After this initial degradation, the solar absorptance stabilizes. However, the measured drop in solar absorptance is significant; in average the solar absorptance drops by 13.8%-points for the proppants, reaching final solar absorptance values of 66–76 % after testing for 4000 h. The same trend is visible for the thermal emittance: in average it drops by 25.7 % but it stabilizes within the first 500 h of

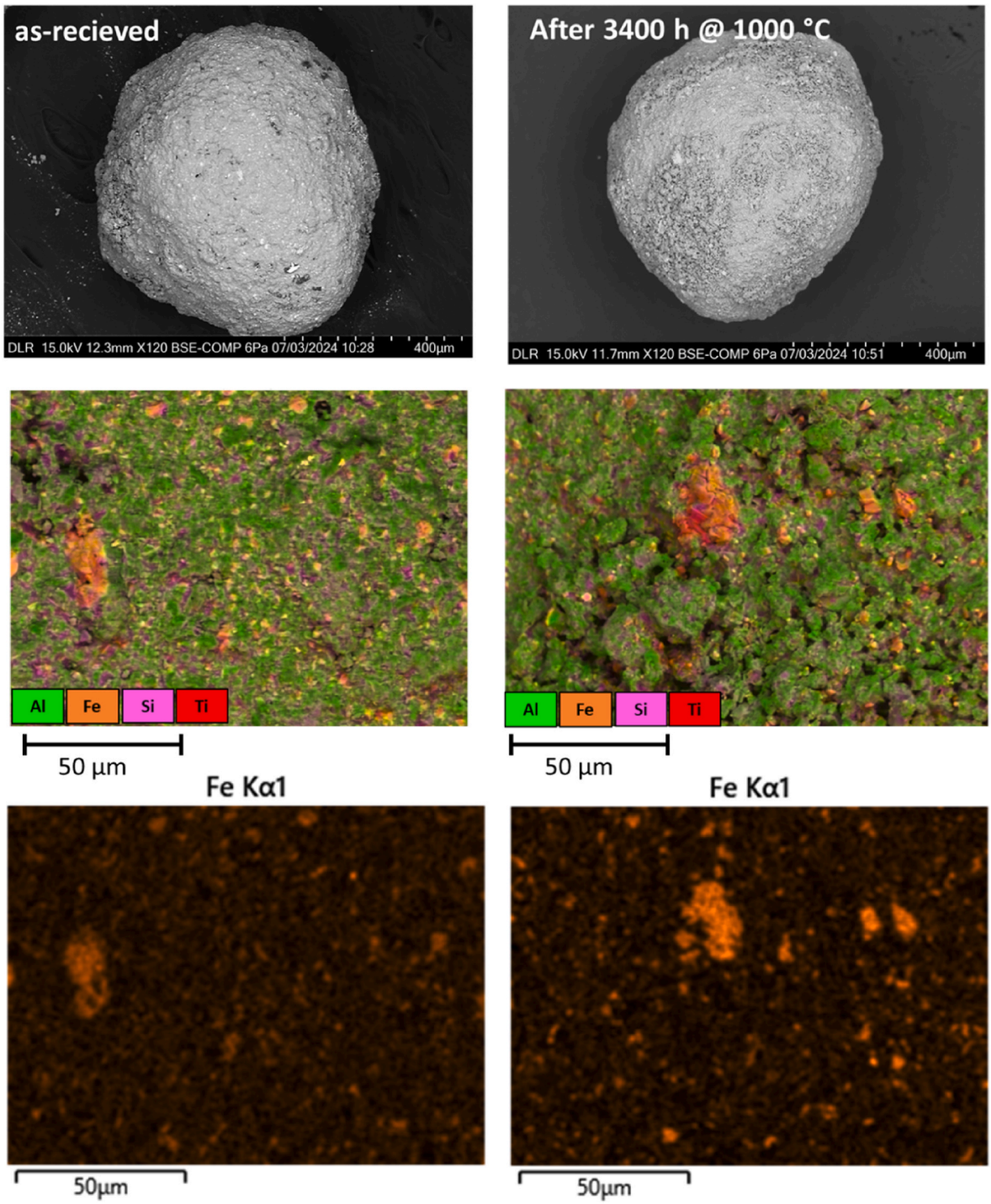

Fig. 10. SEM/EDS analysis of as-received SB30/50 proppants (left) and after 3400 h of exposure to 1000 °C (right). The lower images show Fe-mapping to better visualize the Fe-rich precipitates.

exposure (see Fig. 5).

A similar behavior, although less pronounced as for the proppants, is observed for the novel fused particles. They also undergo a slight optical degradation within the first 500 h of testing. In average, their solar absorptance and thermal emittance values drop by 2.6%-points and 9.5%-points respectively.

On the contrary, the Granulated Gen2, Gen3 and Gen4 particles show very stable optical properties throughout the entire thermal exposure test. Only Gen4 shows minor fluctuations, exhibiting 1.2%-points solar absorptance and 10.6%-points thermal emittance drop after 4000 h of testing.

As general conclusion it can be stated that all novel particle developments outperform the state-of-the-art proppants in terms of optical stability when exposed to 1000 °C. Gen4 particles, which were identified as the most promising ones in terms of commercialization, show a comparable initial solar absorptance of about 83 % to state-of-the-art proppants (SB 30/50, BL 30/50 and IP 30/50). Notably, only the BL 16/30 proppants show a high initial absorptance of 90.5 % despite they consist of the same composition as BL 30/50, which only reaches 83.7 %. This variation is due to slightly different raw materials throughout

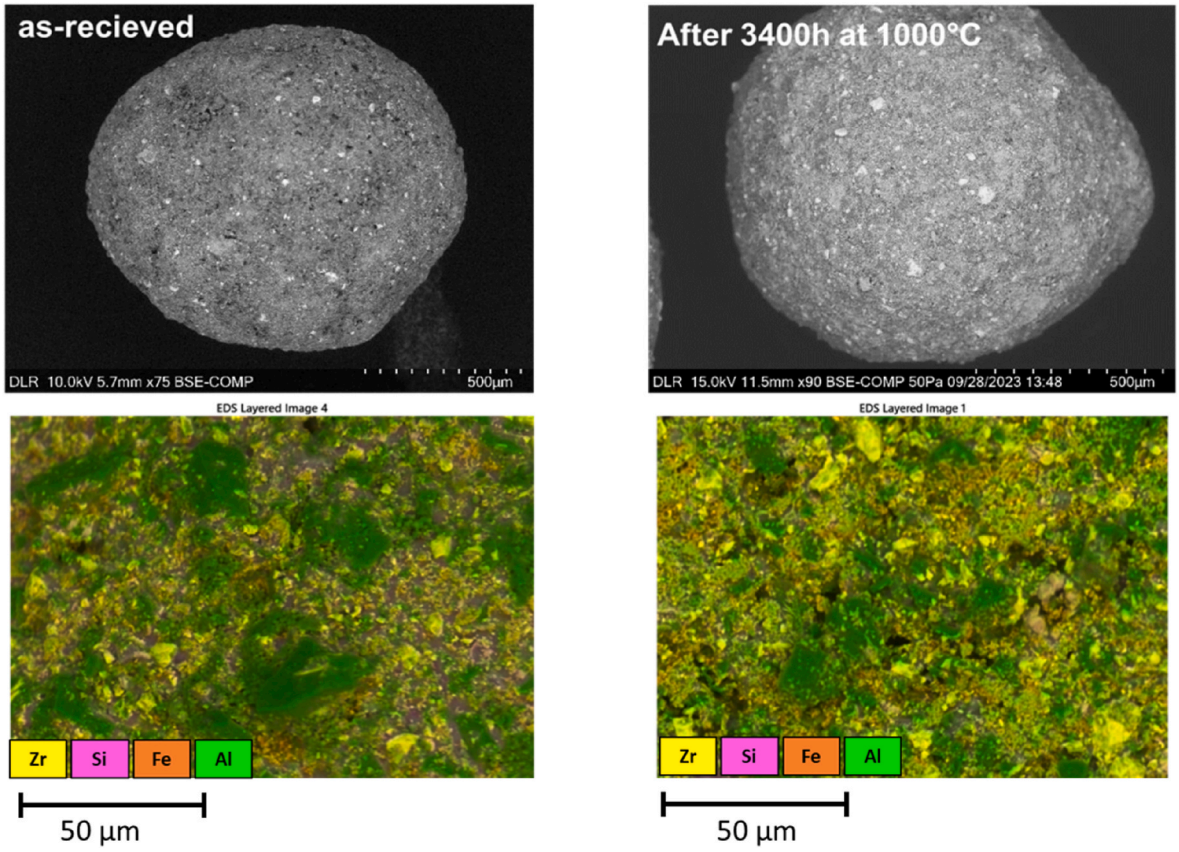

Fig. 11. SEM/EDS analysis of as-received Gen4 particles (left) and after 3400 h of exposure to 1000 °C (right).

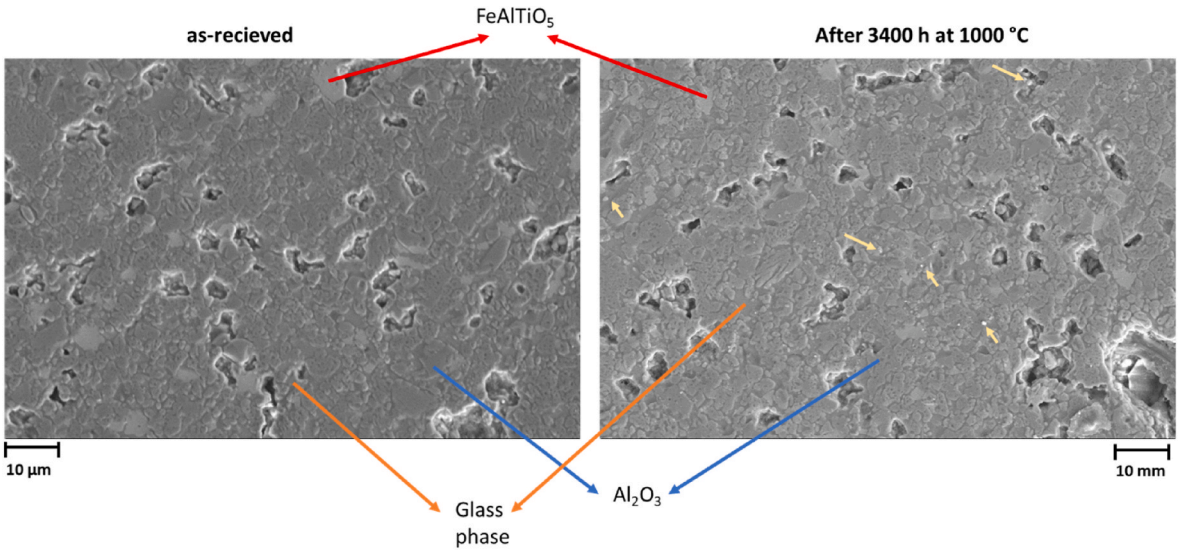

Fig. 12. SEM/EDS cross-section analysis of as-received SB 30/50 proppants (left) and after 3400 h of exposure to 1000 °C (right). The yellow arrows indicate Fe-rich precipitates.

different manufacturing batches. Nevertheless, Gen4 particles maintain solar absorptance above 82 % after the thermal exposure test, whilst BL 16/30 proppants fall down to 75.8 %.

With regards to the coated particles, despite a degradation in solar absorptance of 5%-points of the DFI-coating on Gen3 particles, all particles show stable and promising behavior. CIE-coatings and the DFI-coating on Gen4 maintain solar absorptance above 95 % after testing, which is a significant improvement compared to the state-of-the-art and also compared to the bare granulated particles. DLR-coating also proves excellent temperature stability, however the initial solar absorptance of 92.6 % is lower compared to DFI and CIE.

The color change of the proppants versus the stability of granulated particles can be visually appreciated in Fig. 6, especially when comparing the initial image of SB 30/50 proppants with the one after 500 h of testing.

Fig. 7 shows a direct comparison between state-of-the-art sintered

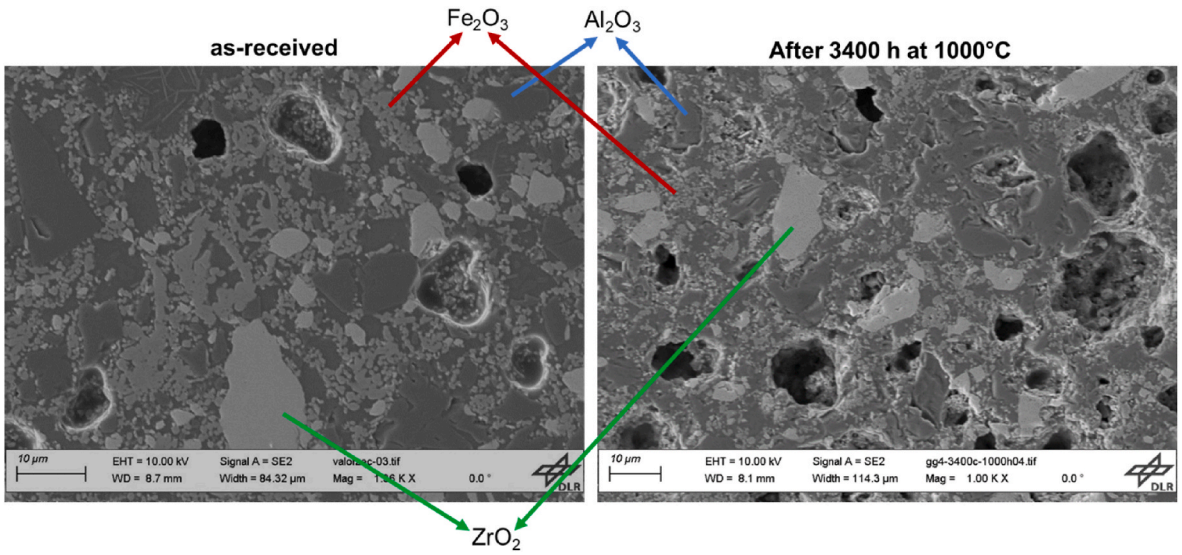

Fig. 13. SEM/EDS cross-section analysis of as-received Gen4 particles (left) and after 3400 h of exposure to 1000 °C (right).

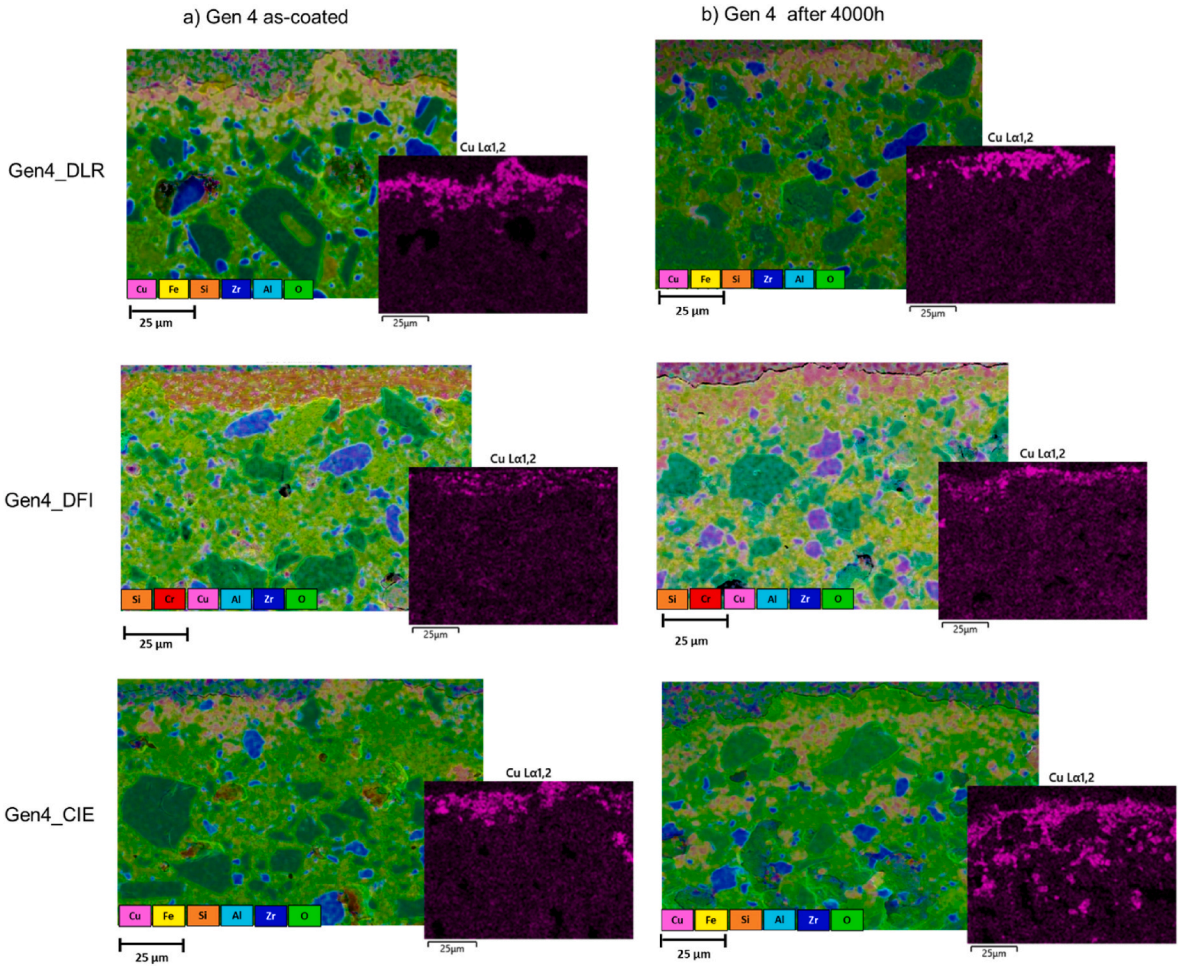

Fig. 14. SEM/EDS cross-section of the three coatings on Gen4 particles a) in initial state; b) after 4000 h of isothermal aging.

bauxite SB 30/50 proppants and granulated Gen4 in terms of spectral absorptance. The graphs remark that Gen4 achieves about one order of magnitude lower solar absorptance loss than SB 30/50 proppants after 4000 h of testing. Also, the spectral emittance shown in Fig. 8 shows significantly less degradation of the particles. The graph points out that the loss in thermal emittance is about three times smaller for the Gen4 particles compared to the sintered bauxite SB 30/50 particles.

In Fig. 9 the evolution of the opto-thermal efficiency computed according to equation (1) is shown. In order to improve readability of the graph, only the most promising particle types and an average of the four

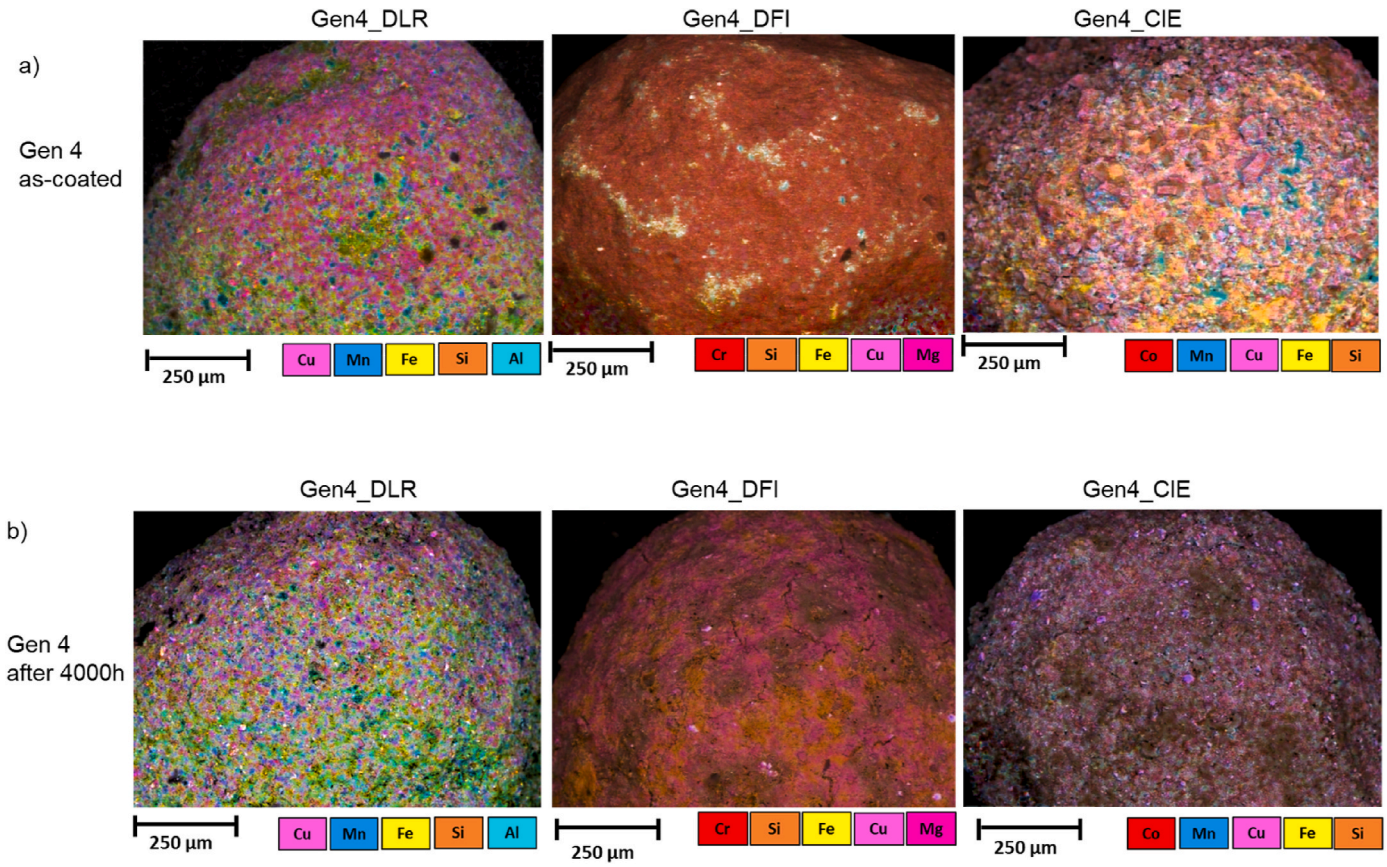

Fig. 15. SEM/EDS surface images of the three coatings on a) Gen4 particles in initial state; b) Gen4 particles after 4000 h of isothermal aging.

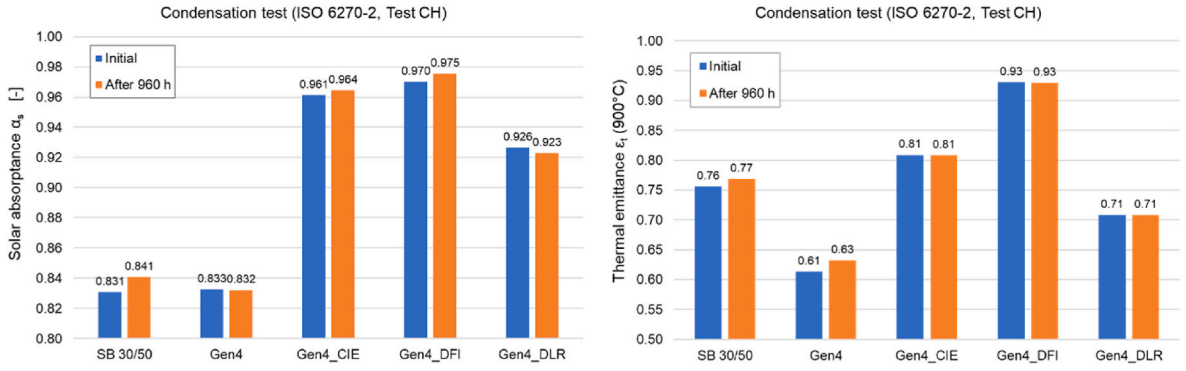

Fig. 16. Solar absorptance (left) and thermal emittance (right) after 960 h of exposure to the condensation test for 5 different particle types.

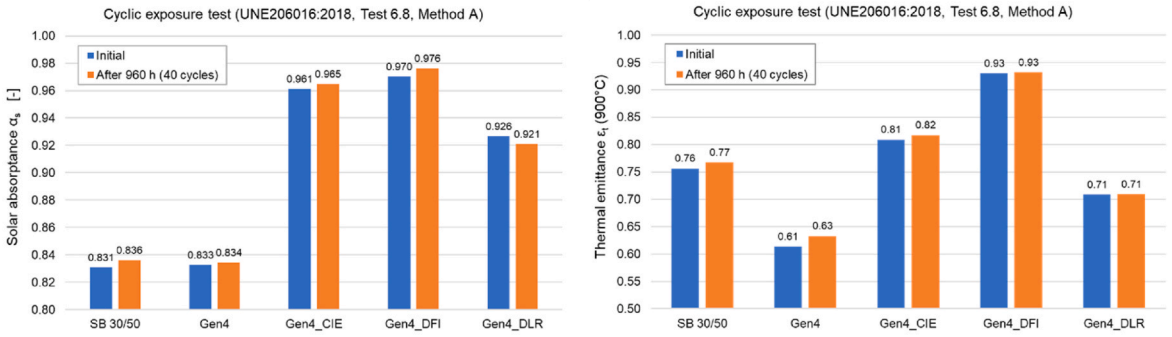

Fig. 17. Solar absorptance (left) and thermal emittance (right) after 960 h/40 cycles of the cyclic exposure test for 5 different particle types.

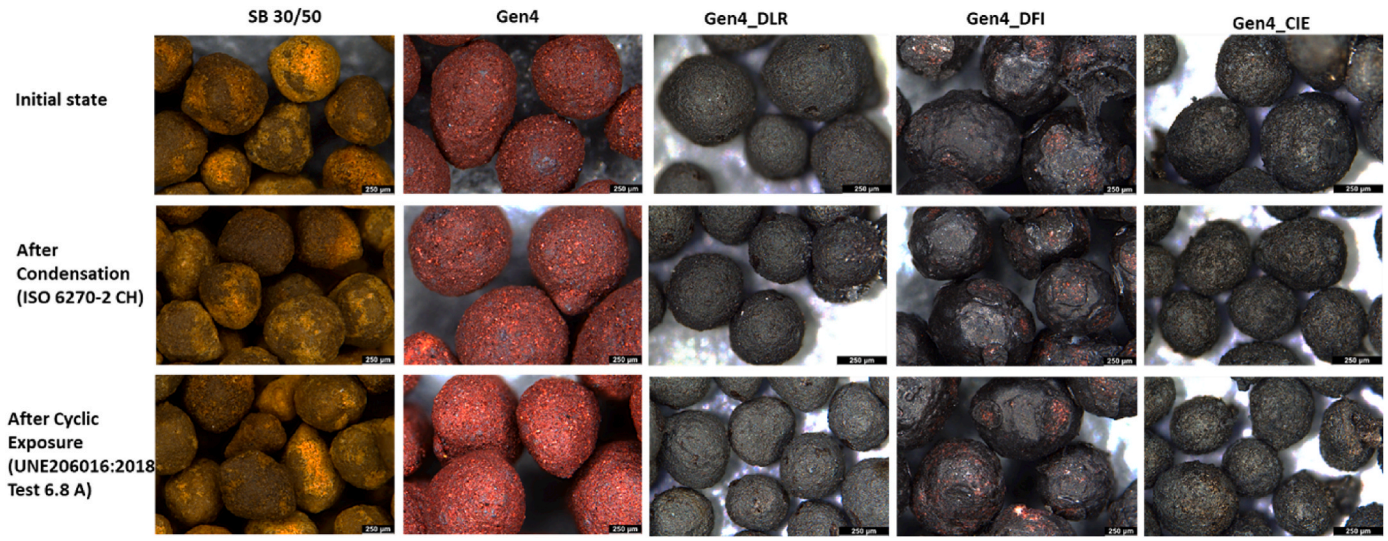

Fig. 18. Light-microscope images before and after environmental exposure testing of the 5 different particle types.

proppant types as reference are displayed. It can be seen that Gen4 particles and proppants part from identical η, but the Gen4 particles maintain their η of ~76.7 % throughout the entire test, while the proppants suffer an opto-thermal efficiency loss of about 11%-points after testing. Also, it becomes visible that all 3 coatings types maintain stable η. The coatings of DFI and CIE achieve values slightly above 87 %, while the η for the DLR coating remains at about 85 %.

Figs. 10 and 11 show SEM images of the surface analysis conducted before and after exposure of the SB 30/50 proppants and the Gen4 particles to 1000 °C for 3400 h. Regarding the SB 30/50 proppants, thermal degradation due to pore coalescence can be observed. Moreover, the formation of Fe-rich precipitates at the surface is also significant (see lower row of Fig. 10). It is likely that these precipitates are responsible for the color change, increasing the light reflection locally and hence leading to lower solar absorptance. On the other hand, Gen4 particles exhibit stable surface characteristics after the exposure to high temperature, which agrees with optical measurements.

Figs. 12 and 13 show the cross-sectional analysis conducted in the SEM for both, SB 30/50 proppants and Gen4 particles. Regarding SB 30/50, the main constituent is alumina (corundum) surrounded by a glassy matrix. The color-giving element, Fe, can be found in the $FeAlTiO_5$ phase, which can be observed as brighter grains in the microstructure. The yellow arrows in Fig. 12 indicate Fe-rich precipitates, in agreement with surface SEM. Other than that, cross-section analysis does not reveal significant changes. Instead, changes and degradation were more pronounced at the surface, which is the reason for color change. Regarding Gen4, the main constituents are Fe_2O_3, alumina, silica and ZrO_2 and it can be concluded that Gen4 presents very stable surface and cross-sectional microstructure characteristics.

Figs. 14 and 15 depict the microstructural and surface changes of the three coating types on Gen 4 particles after 4000 h of exposure to isothermal aging, respectively.

SEM/EDS analysis of thermally aged samples point out coherent findings with the optical measurements. The presence of the coating layer is confirmed with ″Cu″ elemental mapping for all types of coatings after 4000 h aging at 1000 °C, since copper was the common element in all the spinel coatings (see Table 2). None of the coated particles shows a significant change after thermal exposure when compared with as-coated EDS mappings (see Fig. 14a and b). Only the CIEMAT coating exhibits a slight alteration compared to the as-coated initial state by diffusion of the Cu-rich layer into the particle substrate. However, this alteration did not affect the optical properties.

The surface analysis shown in Fig. 15 confirms that the coatings remain intact after the thermal exposure test. Only minimal changes of the surface characteristics are visible for the DFI coating, showing small cracks after the thermal exposure, which might explain their slight reduction in thermal emittance (compare to Fig. 5).

3.2. Environmental exposure tests

The results of the solar absorptance and thermal emittance before and after the environmental exposure tests can be seen in Figs. 16 and 17. All tested particles show excellent resistance against condensation and humidity-freeze conditions. For some particles even a slight increase in solar absorptance and thermal emittance is measured after the test. The differences are within the measurement uncertainty of the equipment. Fig. 18 shows light-microscope images of the different particles before and after environmental exposure testing. No changes in the visual aspect are remarkable. It can be concluded that environmental conditions at ambient temperatures will have negligible impact on the particles or coatings durability.

4. Conclusions

Within this work, the durability of state-of-the-art proppants and novel particles and coatings has been studied. The particles were exposed to an unprecedented long-lasting isothermal exposure test at 1000 °C for 4000 h. In addition, particles and in particular their coatings' resistance to ambient humidity and freezing conditions were tested in accelerated climatic chambers at low temperatures between −40 and 85 °C. All of the tested particles showed no signs of optical degradation in the environmental climate chamber tests and it is expected that humidity or freezing conditions will not impact the particles' performance throughout the lifetime.

As previously reported in literature, it was confirmed within this study that bauxite-based proppants undergo a color change and therefore a reduction in solar absorptance values when exposed to 1000 °C. The degradation was detected in the first optical inspection after 500 h of exposure, but it is likely to happen more quickly (in Ref. [12] it is reported that changes of optical properties on proppants occurred within the first 24 h). After the initial degradation, the solar absorptance and thermal emittance of the proppants stabilize. However, the initial degradation of the four investigated proppant types is quite significant, in average the solar absorptance drops by 13.8%-points, reaching final values of 66–76 % after testing for 4000 h.

On the contrary, the novel granulated particles achieve about one

order of magnitude lower solar absorptance loss compared to the state-of-the-art proppants after 4000 h of testing. Granulated Gen4 particles maintain solar absorptance above 82 % after the thermal exposure test, whilst proppants fall below 76 %. The microstructure and surface of the granulated particles remain stable after testing.

Based on the above-mentioned results and also on the mechanical particle properties determined throughout the H2020 CompassCO2 project, the granulated Gen4 particles were identified as the most promising ones for commercialization. These particles are obtained by granulating waste products from the steel industry and can therefore be produced cost-effectively at a cost of only approx. 1 €/kg. It was demonstrated that in combination with coatings, the solar absorptance can be boosted from 83 up to 97.5 %. All three of the developed coatings for Gen4 particles showed excellent stability under the isothermal and climatic chamber conditions. However, the coating process is estimated to increase the particle cost by about 50–75 €-cents per kg. It remains to be evaluated if the coating cost could be reduced in a large-scale particle production process and if the increase in receiver efficiency will compensate for the higher particle cost. In future work, the durability of the coatings will be investigated under thermocyclic exposure conditions. Furthermore, the attrition and erosion of the coatings will be evaluated at ambient and at operational temperature.

CRediT authorship contribution statement

Florian Sutter: Writing – original draft, Project administration, Methodology, Investigation, Funding acquisition, Data curation, Conceptualization. **Gözde Alkan:** Writing – review & editing, Investigation, Data curation. **Nassira Benameur:** Writing – review & editing, Investigation. **Samuel Marlin:** Writing – review & editing, Investigation. **Gema San Vicente:** Writing – review & editing, Investigation. **Angel Morales:** Writing – review & editing, Investigation. **Tomás Jesus Reche Navarro:** Investigation. **Ana Cleia González Alves:** Investigation. **Lucía Martínez Arcos:** Investigation. **Daniel Benítez:** Project administration, Resources, Validation, Writing – review & editing. **Aránzazu Fernández-García:** Writing – review & editing, Investigation. **Ceyhun Oskay:** Writing – review & editing, Investigation. **Christoph Grimme:** Writing – review & editing, Investigation.

Declaration of competing interest

The authors declare that they have no known competing financial interests or personal relationships that could have appeared to influence the work reported in this paper.

Acknowledgements

This research was financially supported from the European Union's Horizon 2020 Research and Innovation Action (RIA) under grant agreement No. 958418 (CompassCO2 project).

Data availability

Data will be made available on request.

References

[1] C. Ho, A review of high-temperature particle receivers for concentrating solar power, Appl. Therm. Eng. 109 (Part B) (2016) 958–969, https://doi.org/10.1016/j.applthermaleng.2016.04.103. ISSN 1359-4311.
[2] J. Martin, J. Vitko, ASCUAS: A Solar Central Receiver Utilizing a Solid Thermal Carrier, Sandia National Laboratories, 1982. SAND82-8203.
[3] K. Jiang, X. Du, Y. Kong, C. Xu, X. Ju, A comprehensive review on solid particle receivers of concentrated solar power, Renew. Sustain. Energy Rev. 116 (2019) 109463, https://doi.org/10.1016/j.rser.2019.109463. ISSN 1364-0321.
[4] F. Nie, F. Bai, Z. Wang, X. Li, R. Yang, Solid Particle Solar Receivers in the Next-Generation Concentrated Solar Power Plant, EcoMat, 2022 e12207, https://doi.org/10.1002/eom2.12207.
[5] Feng Liang, Mohammed Sayed, Ghaithan A. Al-Muntasheri, Frank F. Chang, Leiming Li, A comprehensive review on proppant technologies, Petroleum 2 (1) (2016) 26–39, https://doi.org/10.1016/j.petlm.2015.11.001. ISSN 2405-6561.
[6] N. Siegel, M. Gross, C. Ho, T. Phan, J. Yuan, Physical properties of solid particle thermal energy storage media for concentrating solar power applications, Energy Proc. 49 (2014) 1015–1023, https://doi.org/10.1016/j.egypro.2014.03.109. ISSN 1876-6102.
[7] N. Siegel, M. Gross, R. Coury, The development of direct absorption and storage media for falling particle solar central receivers, ASME, J. Sol. Energy Eng. 137 (4) (August 2015) 041003, https://doi.org/10.1115/1.4030069.
[8] A. Calderón, C. Barreneche, A.I. Fernández, M. Segarra, Thermal cycling test of solid particles to be used in concentrating solar power plants, Sol. Energy Mater. Sol. Cell. 222 (2021) 110936, https://doi.org/10.1016/j.solmat.2020.110936. ISSN 0927-0248.
[9] A. Palacios, A. Calderón, C. Barreneche, J. Bertomeu, M. Segarra, A.I. Fernández, Study on solar absorptance and thermal stability of solid particles materials used as TES at high temperature on different aging stages for CSP applications, Sol. Energy Mater. Sol. Cell. 201 (2019) 110088, https://doi.org/10.1016/j.solmat.2019.110088. ISSN 0927-0248.
[10] T. Baumann, S. Zunft, Properties of granular materials as heat transfer and storage medium in CSP application, Sol. Energy Mater. Sol. Cell. 143 (2015) 38–47, https://doi.org/10.1016/j.solmat.2015.06.037. ISSN 0927-0248.
[11] M. Diago, A. Crespo Iniesta, A. Soum-Glaude, N. Calvet, Characterization of desert sand to be used as a high-temperature thermal energy storage medium in particle solar receiver technology, Appl. Energy 216 (2018) 402–413, https://doi.org/10.1016/j.apenergy.2018.02.106. ISSN 0306-2619.
[12] J. Roop, S. Jeter, S. Abdel-Khalik, C. Ho, Optical properties of select particulates after high-temperature exposure, ES2014-6504, V001T02A029, https://doi.org/10.1115/ES2014-6504, 2014.
[13] L. Noč, I. Jerman, Review of the spectrally selective (CSP) absorber coatings, suitable for use in SHIP, Sol. Energy Mater. Sol. Cell. 238 (2022) 111625, https://doi.org/10.1016/j.solmat.2022.111625. ISSN 0927-0248.
[14] Z. Zhou, C. He, X. Gao, Recent advances of spectrally selective absorbers: materials, nanostructures, and photothermal power generation, APL Energy 2 (2024) 011503, https://doi.org/10.1063/5.0194976.
[15] K. Xu, M. Du, L. Hao, J. Mi, Q. Yu, S. Li, A review of high-temperature selective absorbing coatings for solar thermal applications, J. Materiom. 6 (1) (2020) 167–182, https://doi.org/10.1016/j.jmat.2019.12.012. ISSN 2352-8478.
[16] S. Caron, Y. Binyamin, M. Baidossi, A. Agüero, C. Hildebrandt, M. Galetz, F. Sutter, Durability testing of solar receiver coatings: experimental results for T91 and VM12 substrates, AIP Conf. Proc. 2303 (2020) 150006, https://doi.org/10.1063/5.0028772.
[17] R. Harzallah, M. Larnicol, C. Leclercq, A. Herbein, F. Campana, Development of high performances solar absorber coatings, AIP Conf. Proc. 2126 (2019) 030026, https://doi.org/10.1063/1.5117538.
[18] J. Torres, K. Tsuda, Y. Murakami, Y. Guo, S. Hosseini, C.A. Asselineau, M. Taheri, K. Drewes, A. Tricoli, W. Lipinski, J. Coventry, Highly efficient and durable solar thermal energy harvesting via scalable hierarchical coatings inspired by stony corals, Energy Environ. Sci. 15 (2022) 1893–1906, https://doi.org/10.1039/D1EE03028K.
[19] B. Gobereit, L. Amsbeck, C. Happich, M. Schmücker, Assessment and improvement of optical properties of particles for solid particle receiver, Sol. Energy 199 (2020) 844–851, https://doi.org/10.1016/j.solener.2020.02.076. ISSN 0038-092X.
[20] J. Wu, J. Du, J. Wu, X. Du, Modification of high temperature radiation absorption properties of solid particles with surface coating, Sol. Energy Mater. Sol. Cell. 263 (2023) 112567, https://doi.org/10.1016/j.solmat.2023.112567. ISSN 0927-0248.
[21] T. Galiullin, B. Gobereit, D. Naumenko, R. Buck, L. Amsbeck, M. Neises-von Puttkamer, W.J. Quadakkers, High temperature oxidation and erosion of candidate materials for particle receivers of concentrated solar power tower systems, Sol. Energy 188 (2019) 883–889, https://doi.org/10.1016/j.solener.2019.06.057. ISSN 0038-092X.
[22] K. Kant, R. Pitchumani, Erosion wear analysis of heat exchange surfaces in a falling particle-based concentrating solar power system, Sol. Energy Mater. Sol. Cell. 266 (2024) 112629, https://doi.org/10.1016/j.solmat.2023.112629. ISSN 0927-0248.
[23] R. Knott, D. Sadowski, S. Jeter, S. Abdel-Khalik, H. Al-Ansary, A. El-Leathy, High temperature durability of solid particles for use in particle heating concentrator solar power systems. https://doi.org/10.1115/ES2014-6586, 2014.
[24] G. Alkan, P. Mechnich, J. Pernpeintner, Improved performance of ceramic solar absorber particles coated with black oxide pigment deposited by resonant acoustic mixing and reaction sintering, Coatings 12 (2022) 757, https://doi.org/10.3390/coatings12060757.
[25] G. Alkan, P. Mechnich, J. Pernpeintner, Using an Al-incorporated deep black pigment coating to enhance the solar absorptance of iron oxide-rich particles, Coatings 13 (2023) 1925, https://doi.org/10.3390/coatings13111925.
[26] M. Farchado, G. San Vicente, N. Barandica, F. Sutter, G. Alkan, D. Sánchez-Señorán, A. Morales, Performance improvement of CSP particle receivers by depositing spinel absorber coatings, Sol. Energy Mater. Sol. Cell. 266 (2024) 112681, https://doi.org/10.1016/j.solmat.2023.112681. ISSN 0927-0248.
[27] ISO 6270-2:2017-11 Paints and Varnishes - Determination of Resistance to Humidity - Part 2: Condensation (In-cabinet Exposure with Heated Water Reservoir).
[28] UNE 206016:2018 Reflector Panels for Concentrating Solar Technologies.
[29] F. Sutter, J. Pernpeintner, S. Caron, A. Morales, G. San Vicente, A. Fernández-García, M. Montecchi, A. Calderón, M. Majó, A.I. Fernández, P. Davenport, T. Farrell, C. Ho, Method to evaluate the reflectance, absorptance and emittance of particles for concentrating solar power technology, SolarPACES guideline,

available online:, Version 1, May 2022. https://www.solarpaces.org/wp-content/uploads/SolarPACES-Particle-Reflectance-Guideline-logo-update.pdf.
[30] F. Sutter, M. Montecchi, A. Morales, G. San Vicente, A. Fernández-García, J. Pernpeintner, T. Reche-Navarro, L. Martinez-Arcos, J. Wette, A. Calderon, M. Majó, A.I. Fernández, P. Davenport, T. Farrell, C. Ho, Round robin test of absorptance and emittance of particles for CSP. SolarPACES Conference Proceedings, 2022, https://doi.org/10.52825/solarpaces.v1i.629.
[31] IEC 60904-3:2019 Photovoltaic Devices - Part 3: Measurement Principles for Terrestrial Photovoltaic (PV) Solar Devices with Reference Spectral Irradiance Data.